ERIES-PASFIT Test Report

Long-Term Performance Assessment of Base Isolated Buildings through Field Testing

User Group:

Sucuoglu Haluk[1], Calvi Paolo[2], Rapone Aldo[3], Becker Tracy[4], Ozcamur Ugurcan[5], Kaatsiz Kaan[6], Alici Firat Soner[7]

Research Infrastructure staff:

Lanese Igor[7], Rizzo Parisi Elisa[7], Dacarro Filippo[7], Bottoni Alberto[7], Gerard O'Reilly[3]

[1] Department of Civil Engineering Middle East Technical University, Ankara, Turkey

[2] Civil and Environmental Engineering University of Washington, Seattle, Washington

[3] IUSS, Pavia, Italy

[4] Department of Civil and Environmental Engineering University of California, Berkeley, California

[5] TIS Technological Isolation Systems, Ankara, Turkey

[6] Baskent University, Ankara, Turkey

[7] Eucentre, Pavia, Italy

Order protocol

2022.EUC.003

Via Ferrata 1, 27100 Pavia, Italy
Tel. +39.0382.516911 Fax. +39.0382.529131
http://www.eucentre.it
email: info@eucentre.it

ERIES-PASFIT Test Report

Long-Term Performance Assessment of Base Isolated Buildings through Field Testing

Report ID: **ERIES-PASFIT**

Document	Written pages:	Total pages:
Test Report	22	24

Issue:	Revision:	Revision:	Revision:
14th May 2026	-	-	-

File Name:	protocol / order
ERIES-PASFIT_ Test_Report.pdf	2022.EUC.003

Description

The present report provides a short description of the ERIES-PASFIT Project and its experimental campaign carried out in Arischia, Italy in October 2024 using the EUCENTRE's Mobile Laboratory (or MOBILAB) within the framework of ERIES (www.eries.eu).

The ERIES project (Engineering Research Infrastructures for European Synergies) is funded by the European Commission's Horizon Europe program. Coordinated by the Scuola Universitaria Superiore IUSS Pavia in Italy, it has a budget of €11.6 million and has a four-year duration, from 2022 to 2026.

ERIES aims to provide transnational access to advanced research infrastructures in structural, seismic, wind, and geotechnical engineering. The project seeks to enhance resilience against natural hazards such as earthquakes and extreme winds by fostering innovative and sustainable solutions to mitigate economic losses and social disruptions. Additionally, it develops new technical standards and methodologies to improve built environment safety and supports frontier research through international collaboration.
The ERIES network includes 13 partners from 8 countries across Europe and North America: IUSS Pavia and Eucentre Foundation (Italy), University of Patras (Greece), Aristotle University of Thessaloniki (Greece), Laboratório Nacional de Engenharia Civil (Portugal), Centre de recherche CEA Paris-Saclay (France), Institute of Earthquake Engineering and Engineering Seismology (North Macedonia), Joint Research Centre (Italy), University of Bristol (United Kingdom), University of Genova (Italy), Western University (Canada), Eindhoven University of Technology (Netherlands) and CSTB Nantes (France).

In this Report, a description of the ERIES-PASFIT Project, materials and specimens, test setup and tests carried out is provided.

Table of Contents

1 Introduction ... 8
2 Case Study Characterization ... 8
2.1 C.A.S.E. Project ... 8
2.2 Case-study building ... 9
3 Experimental setup ... 12
3.1 Instrumentation ... 16
3.2 Testing protocol ... 17
4 Conclusion ... 19
References ... 19
Annex A ... 20

Index of Tables

Table 1: Complete testing protocol of experimental campaign. ... 18
Table 2: List of instruments ... 20
Table 3: List of instruments of external acquisition ... 21
Table 4: List of instruments of external acquisition post test 7 ... 21

Index of Figures

Figure 1: Location of case study building. ... 10
Figure 2: Case study floor plan view of first and second floor. ... 11
Figure 3: Technical drawings of North and West view. ... 11
Figure 4: Technical drawings and nominal parameter of ALGA bearing. ... 12
Figure 5: Isolation bearings placed at the top of the hollow steel column. ... 12
Figure 6: Self-reacting frame anchored to steel columns. ... 13
Figure 7: MOBILAB main components ... 14
Figure 8: Disposition of self-reacting frame on the steel columns pattern. ... 15
Figure 9: Self-reacting frame components and force pattern. ... 15
Figure 10: Exploded view of the U-frame. ... 15
Figure 11: Abaqus FEM model created for detailed analysis of steel frame connections. ... 16
Figure 12: Technical drawings and photos of instrumentation layout in case-study. ... 17
Figure 13: Displacement input of 100% for the ground motion based tests. ... 18
Figure 14: Instrumentation layout – basement level. ... 22
Figure 15: Instrumentation layout – plate level. ... 22
Figure 16: Instrumentation layout – slab level 1. ... 23
Figure 17: Instrumentation layout – slab level 2. ... 23
Figure 18: Instrumentation layout – slab level 3. ... 24

1 Introduction

Base isolation has emerged as one of the most effective and elegant strategies for protecting infrastructure and their contents under seismic loading, both in the context of new construction and in the retrofit of existing systems. The benefits of base isolation are twofold: first, by increasing the fundamental period of vibration and adding damping, the structural response is shifted into a more favourable regime and overall forces are lowered, and second, by changing the mode shape of the structure, displacement is concentrated into the isolation layer, greatly minimizing story drifts.
However, understanding of the performance of isolated buildings is primarily based on component level testing of new isolation bearings. Less well understood is the performance of large groups of isolators, each of which may have a slight variation in properties within the allowable design limits. Furthermore, interaction with the sub- and superstructure have the potential to change the demands on the bearing. On top of this, it is understood that the long-term beahvior of a base isolation system may differ significantly from its original as-designed behavior. While this has been explored on rare occasions for individual aged bearings, generating sparse data points, there are no previous studies testing system-level aged isolated buildings.
ERIES- PASFIT will conduct full-scale in-situ testing of buildings; base isolated via laminated rubber bearings and friction pendulum (FP) systems that have been in service for approximately 15 years. The results of these field tests will be the first of their kind, and will be used to fill important research gaps pertaining to the characterization of the response and performance of base isolated buildings, including aspects of system-level response in conjunction with aging, deterioration and more generally, variability of the mechanical properties of the isolation devices. Thus, this will have important implications on base isolation design, assessment and modelling strategies.

The work presented in this report is part of the ERIES project, which provides transnational access to leading experimental facilities. This experimental program, named ERIES-PASFIT (Long-Term Performance Assessment of Base Isolated Buildings through Field Testing), was a multiteam work composed by the Middle East Technical Universities (Ankara, Turkey) in collaboration with the University of Washington (Seattle, US), University of California (Berkeley, US), EUCENTRE Foundation, and IUSS Pavia (Italy).

A dynamic full-scale shake-table testing campaign was conducted on an existing building of the CASE Project in the complex of Arischia, Italy, using the innovative Mobile Laboratory MOBILAB of the EUCENTRE Foundation in Pavia, Italy.
Detailed primary results of the testing setup, the isolation system and the superstructure behavior are available in the articles [1].

2 Case Study Characterization

2.1 C.A.S.E. Project

Following the 2009 L'Aquila earthquake in Italy, the C.A.S.E. (Complessi Antisismici Sostenibili ed Ecocompatibili) Project [2-3] was launched to construct 185 base-isolated buildings intended to accommodate approximately 12,000 residents displaced by the event. These seismically isolated structures are distributed across 20 complexes surrounding the city and typically consist of a three-story superstructure supported by a reinforced concrete transfer slab. This slab is elevated on seismic isolation bearings seated atop steel or reinforced-concrete columns. The columns are generally arranged according to a 6 m × 6 m orthogonal grid and are anchored to reinforced concrete foundations directly interfacing with the ground.

The buildings were constructed using various structural systems, resulting in 92 timber-frame, 57 reinforced-concrete, and 36 steel-frame superstructures. This diversification in construction typology facilitated expedited reconstruction by engaging different industrial sectors in parallel; however, all buildings share an identical substructure typology separated by a seismic isolation layer. The typical total superstructure weight ranges from 30 to 40 MN, corresponding to an average axial load of approximately 1 MN per column. Two primary isolation technologies were implemented: (i) elastomeric bearings combined with multidirectional sliding pot bearings and (ii) single- or double-curvature Friction Pendulum (FP) bearings.

The structure designated “Building 20.4” was selected from among the unoccupied buildings based on its compatibility with the available experimental equipment and its representative physical characteristics—particularly mass and geometric configuration—relative to the full building stock. Building 20.4 is one of four structures constructed in Arischia, a small village near L’Aquila.

2.2 Case-study building

The case-study structure, “Building 20.4” (see Figure 1, Figure 2 and Figure 3), is a three-story residential timber building composed of three interconnected wings connected via two stair–elevator cores and comprising six residential units per floor. The two lateral wings have plan dimensions of 12 m × 6 m, whereas the central wing is four times larger, measuring 12 m × 24 m. Story heights range between 3.13 m and 3.20 m, and the attic space reaches a maximum height of approximately 2.5 m. The total structural height—from the top surface of the reinforced concrete isolation slab to the ridge of the pitched roof—is approximately 12 m.

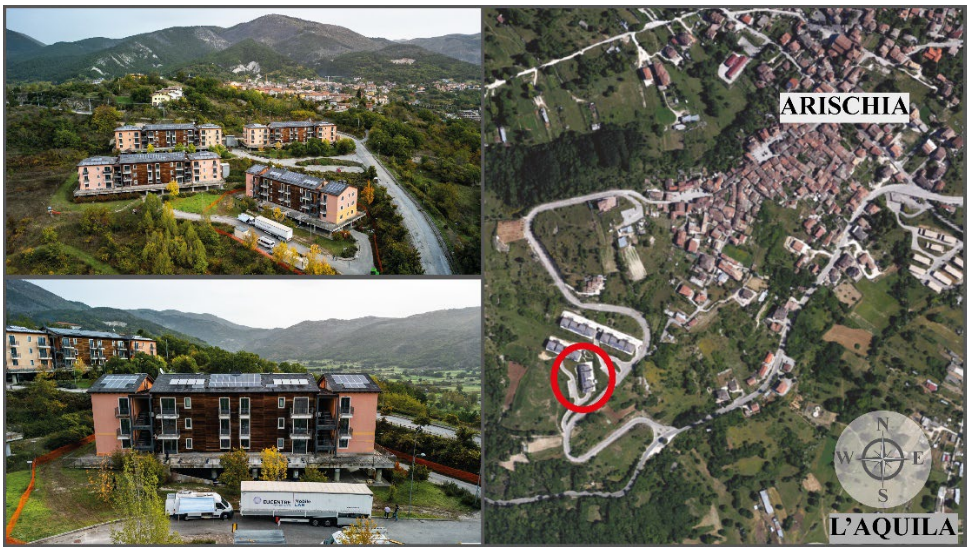

Figure 1: Location of case study building.

The superstructure rests on a 500 mm thick, 21 m × 45 m reinforced concrete slab supported by 32 hollow steel columns with an external diameter of 800 mm and height of 2.45 m. Plan and elevation views and other relevant dimensions appear in Figure 2 and Figure 3. The structural mass of the timber superstructure is approximately 600 tonnes. Including the concrete slab, the total dead mass increases to about 1500 tonnes, excluding live loads. The building's fixed-base fundamental period is estimated to be 0.26 s, and its design seismic base shear corresponds to 0.2W, where W is the seismic weight. Building 20.4, approximately 20% smaller in plan area than a typical C.A.S.E. building, was selected for testing due to its lower mass and overall dimensions, enabling increased testing flexibility (e.g., larger displacements, higher velocities, and accelerations).

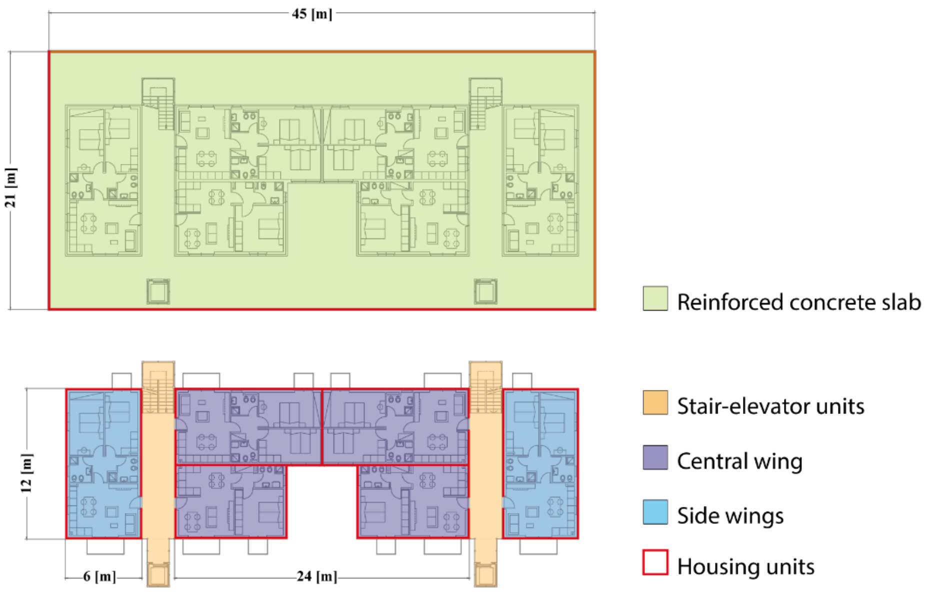

Figure 2: Case study floor plan view of first and second floor.

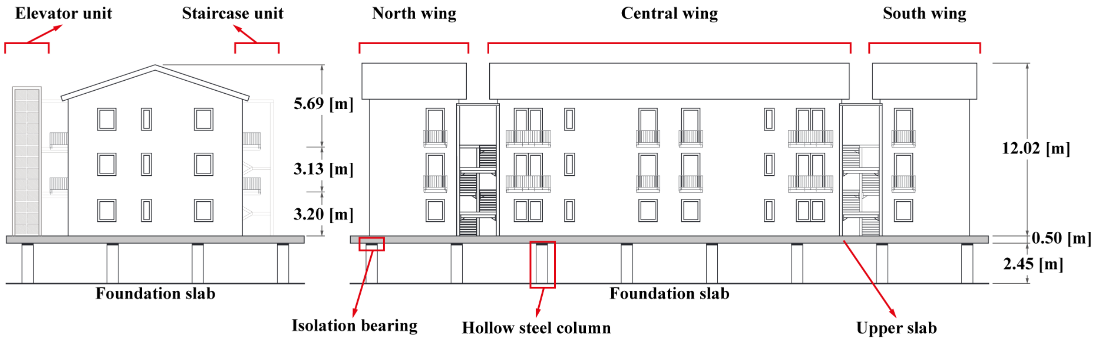

Figure 3: Technical drawings of North and West view.

The structure is equipped with a base isolation system comprising 32 single-curvature Friction Pendulum bearings manufactured by ALGA [2]. The nominal properties of each isolator include a friction coefficient μ = 5%, an effective radius of curvature Req = 3500 mm, and a maximum displacement capacity d_max = 260 mm. A typical ALGA bearing is shown in Figure 4, together with its nominal mechanical parameters. Based on the design properties and total mass, the isolated structure exhibits an estimated secant-period of approximately 3 s. Some images of an in-situ friction pendulum bearing is shown in Figure 5.

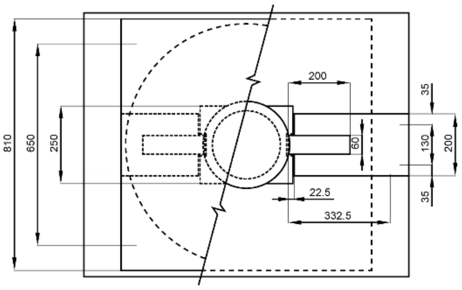

Isolators Nominal Values		
L	810	[mm]
D	800	[mm]
D_{pad}	250	[mm]
R_{eq}	3500	[mm]
μ	5.0	[%]
d_{max}	260	[mm]

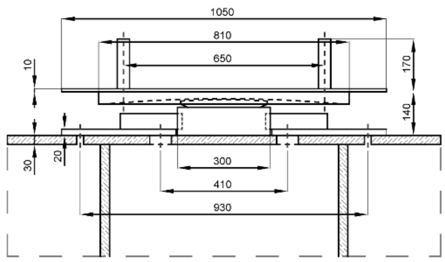

Figure 4: Technical drawings and nominal parameter of ALGA bearing.

Figure 5: Isolation bearings placed at the top of the hollow steel column.

3 Experimental setup

The case-study building was subjected to horizontal loading in the E–W direction by applying push–pull forces to the underside of the reinforced concrete slab supporting the superstructure using four dynamic actuators with 1000 kN capacity each. To achieve this, a dedicated on-site experimental configuration was implemented utilizing EUCENTRE's MOBILAB system in combination with four self-reacting steel frames designed to transfer actuator reaction forces to the foundation (Figure 6).

Figure 6: Self-reacting frame anchored to steel columns.

The main components of the MOBILAB system are shown in Figure 7 and include:

- Four hydraulic actuators capable of delivering dynamic forces up to 1000 kN and ±250 mm displacement to simulate seismic-type loading;
- A hydraulic system comprising pumps, reservoirs, accumulators, and hydraulic lines required to supply the actuators;
- A control unit equipped with a digital controller for synchronizing actuator commands and managing data acquisition;
- An 800 kVA power unit ensuring operational autonomy.

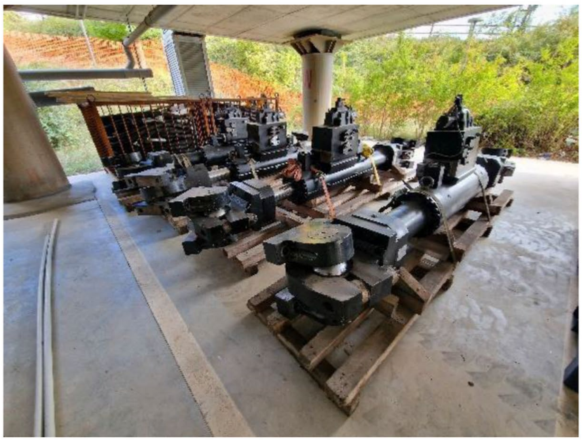

(a) MOBILAB Actuators

(b) MOBILAB external view

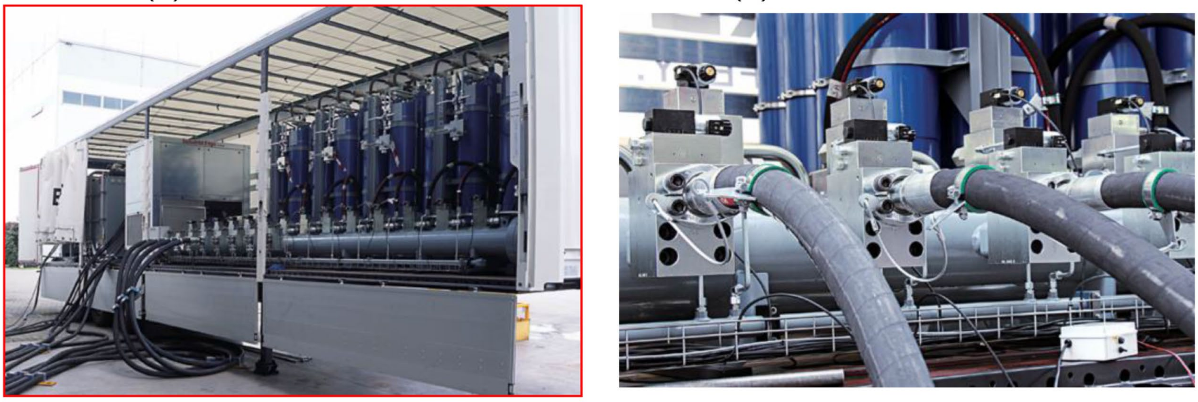

(c) MOBILAB hydraulic system

Figure 7: MOBILAB main components

The steel reaction frames were specifically designed to anchor the four actuators and transfer their maximum force output safely while preventing damage to the foundation. Modularity was included to facilitate transportation and assembly on testing site. The actuators were installed between the four central column pairs on the West façade (Figure 8).

Each reaction frame was connected to three columns aligned with the actuator axis, as illustrated in Figure 9. Since direct anchorage to the isolated slab was not feasible, a custom fastening system was designed to transfer actuator loads while accommodating slab displacements. The reaction frame was therefore subdivided into two components flanking each actuator: (i) an upper component anchored to the isolated slab and (ii) a lower component anchored to the supporting steel columns. The lower component consisted of a truss system transferring forces to the column bases without causing overstress, utilizing retention rings at the base of the outer columns and at the top of the central column. Paired steel profiles were installed between the rings to achieve uniform stress distribution and avoid local instabilities. Figure 9 shows the load transfer mechanism during push (blue) and pull (red) phases. The upper U-shaped frame accommodated relative displacement between slab and columns and consisted of two longitudinal members and a transverse actuator beam anchored using post-tensioned bars, relying on friction-based connections to sustain applied forces (Figure 10).

Bolted connections were used extensively to accommodate fabrication and assembly tolerances. The column-connected frame was segmented for transport, with each of the three rings fabricated as two halves and equipped with spacers to compensate for geometric deviations. The rings were connected by a bolted truss assembly composed of HEB profiles and L-shaped bracing designed against buckling. Due to the unique nature of the setup and MOBILAB equipment, the design was validated through detailed finite element analyses performed in Abaqus [4] using solid elements. These analyses verified the adequacy of stress distribution and prevented column overstress (Figure 11). Full-penetration welds were used in the ring assemblies to ensure continuity and structural capacity.

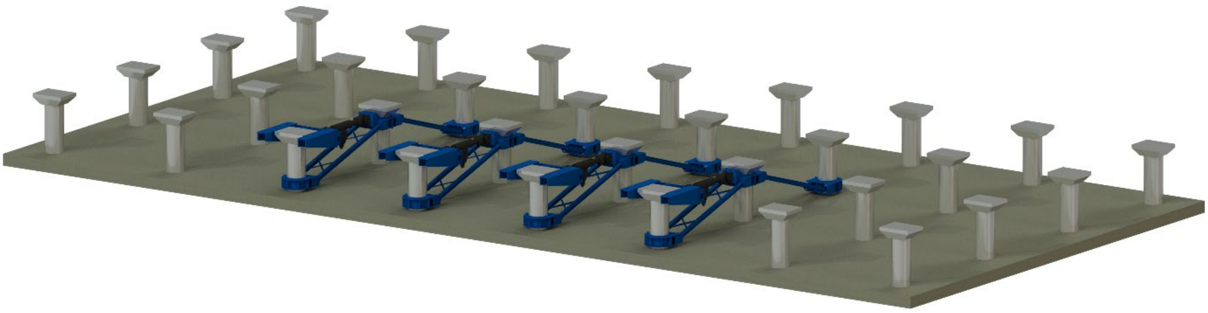

Figure 8: Disposition of self-reacting frame on the steel columns pattern.

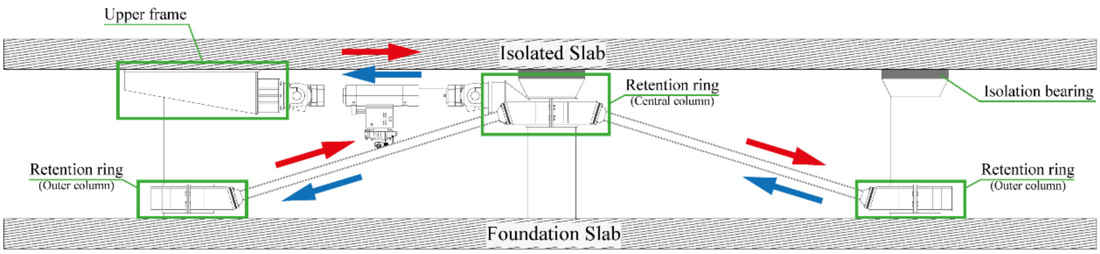

Figure 9: Self-reacting frame components and force pattern.

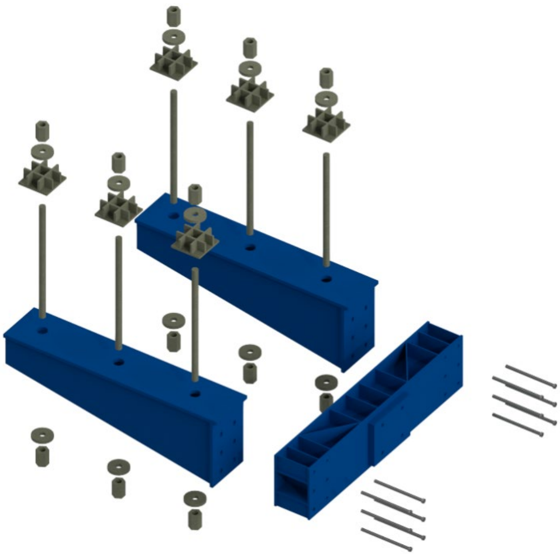

Figure 10: Exploded view of the U-frame.

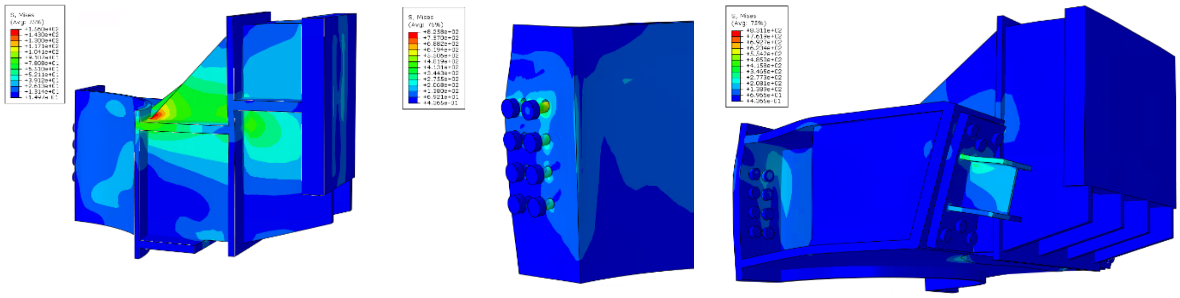

Figure 11: Abaqus FEM model created for detailed analysis of steel frame connections.

3.1 Instrumentation

The structural response was recorded using a comprehensive instrumentation layout, including load cells, tri-axial accelerometers, and linear variable displacement transducers (LVDTs), installed at multiple locations on the slab and superstructure to allow continuous time-history monitoring. High-resolution video recordings of selected isolation bearings were obtained to assess differential displacements. Additional fixed-camera and UAV footage, as well as pre- and post-test visual inspections with detailed photographic documentation, were collected.

A total of 49 channels were recorded: 23 connected to the MOBILAB controller (comprising all displacement transducers, 15 of which were assigned to setup control) and 26 connected to an external acquisition system (including all accelerometers and two string potentiometers used for interstory drift measurements). The instrumentation layout is visible in Figure 12 for slab level and superstructure.

Slab displacement relative to the ground in the E–W direction was monitored using four string potentiometers (±1000 mm stroke). LVDT 1 and LVDT 4 measured displacements at the NW and SW slab corners, respectively; LVDT 2 and LVDT 3 monitored slab movement along the east side, aligned with actuator axes, positioned midway between Actuators 1–2 and Actuators 3–4, respectively. Two additional tracers (Tracer 1 and Tracer 2) measured slab-to-column relative displacements at two critical locations. Two potentiometers (±250 mm stroke) monitored slab displacements in the transverse (N–S) direction: LVDT 5 at the NW and LVDT 6 at the SW slab corners. Two dial gauges (±25 mm) measured vertical slab movements. Deformations of the self-reacting steel frames and columns were also monitored to ensure that applied forces did not induce excessive localized deformation. Two tri-axial accelerometers were installed on each floor at the NW (Acc. 2,4,6,8) and SW (Acc. 1,3,5,7) slab and superstructure corners. These devices had amplitude ranges of ±2 g (slab, first floor, and second floor) and ±6 g (roof level), operating frequencies from DC to 200 Hz, and a dynamic range of 155 dB. Although the primary focus of testing was the isolation system, accelerometers were also installed at the center of each floor diaphragm.

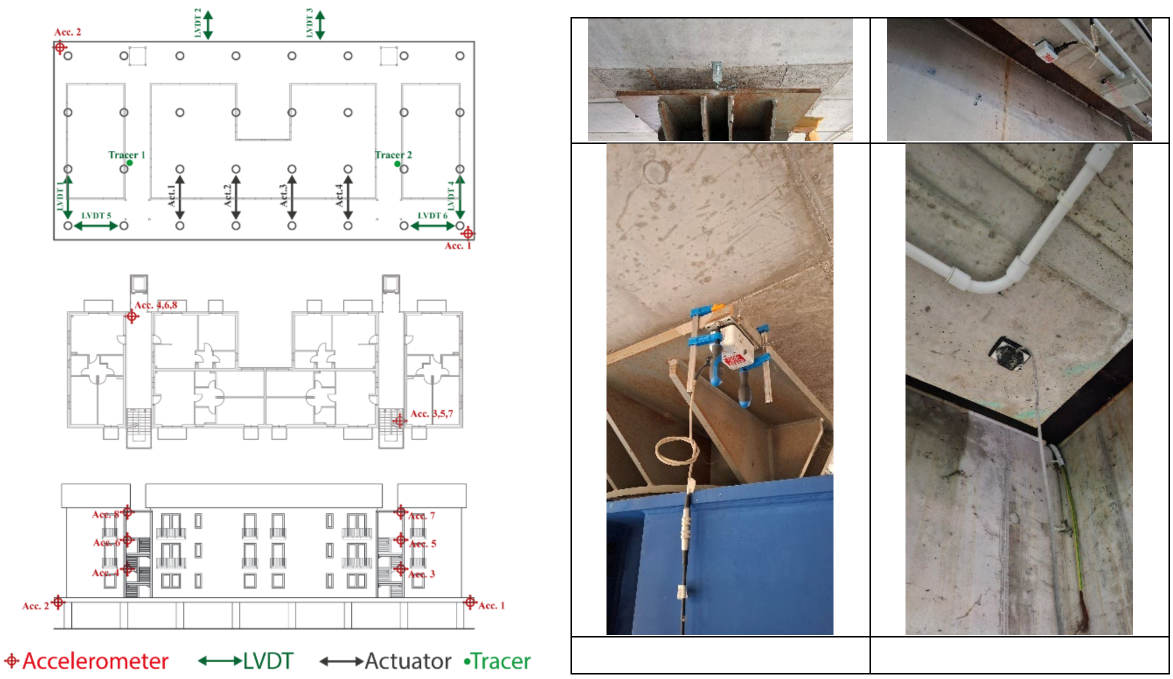

Figure 12: Technical drawings and photos of instrumentation layout in case-study.

3.2 Testing protocol

The testing protocol was designed primarily to evaluate the performance of the base isolation system. Accordingly, displacement-controlled three-cycle sinusoidal loading histories with varying amplitudes and velocities were selected, consistent with EN 15129 provisions [5] used in Europe for laboratory characterization of seismic isolation devices. The displacement amplitudes ranged from ±50 mm to ±200 mm (25%–100% of the design displacement of 200 mm), and the applied loading velocities ranged from 50 mm/s up to 250 mm/s. This range of cyclic motions enabled evaluation of the system response across a variety of excitation frequencies.

Additionally 9 ground motion based tests were performed in order to evaluate the isolation system and superstructure behavior under a real seismic load. All these tests are based on the record of a real ground motion and scaled for the compatibility with the NTC18 [6] spectra for the site. In Figure 13 is visible the 100% input of these tests.

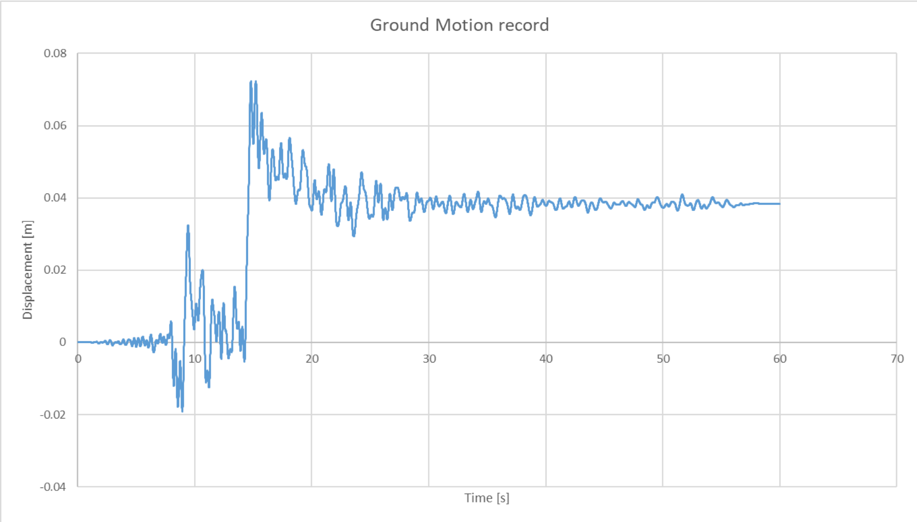

Figure 13: Displacement input of 100% for the ground motion based tests.

The eighteen tests summarized in the Table 1 are discussed herein. In this table, are visible from left to right, the date of the test, the test number, the file name, the test type, the amplitude, the peak velocity, the number of cycles and the sampling of record. In the case of Displacement Histories tests, in the amplitude column are visible the scale factor of the ground motion visible in Figure 13.

Table 1: Complete testing protocol of experimental campaign.

Date	# Test	File Name	Test type	Amplitude [mm]	Velocity [mm/s]	N° cycles	SR (Hz)
11/10/2024	1	T6_sine_50mm_0_159Hz	sine	50	50	3	256
11/10/2024	2	T11_sine_50mm_0_318Hz	sine	50	100	3	256
11/10/2024	3	T16_sine_50mm_0_637Hz	sine	50	200	3	256
12/10/2024	4	T16_sine_50mm_0_637Hz_B	sine	50	200	3	256
12/10/2024	5	T7_sine_100mm_0_08Hz	sine	100	50	3	256
12/10/2024	6	T12_sine_100mm_0_159Hz	sine	100	100	3	256
12/10/2024	7	T17_sine_100mm_0_318Hz	sine	100	200	3	256
12/10/2024	8	T9_sine_200mm_0_04Hz	sine	200	50	3	256
12/10/2024	9	T14_sine_200mm_0_08Hz	sine	200	100	3	256
12/10/2024	10	T14B_sine_200mm_0_119Hz	sine	200	150	3	256
12/10/2024	11	T19_sine_200mm_0_159Hz	sine	200	200	3	256
12/10/2024	12	T2_sine_130mm_0_061Hz	sine	130	50	1	256
12/10/2024	13	T3_sine_130mm_0_122Hz	sine	130	100	1	256
12/10/2024	14	T4_sine_150mm_0_212Hz	sine	150	200	1	256
12/10/2024	15	T5_sine_150mm_0_265Hz	sine	150	250	1	256
12/10/2024	16	T21_sine_50mm_0_796Hz	sine	50	250	3	256
14/10/2024	17	T19_sine_200mm_0_159Hz_B	sine	200	200	3	256
14/10/2024	18	T23_sine_150mm_0_265Hz	sine	150	250	3	256
14/10/2024	19	T24_sine_200mm_0_199Hz	sine	200	250	2	256
14/10/2024	20	T22_sine_100mm_0_398Hz	sine	100	250	3	256
14/10/2024	21	T24_sine_200mm_0_199Hz_B	sine	200	250	2	256
14/10/2024	22	T19_sine_200mm_0_159Hz_C	sine	200	200	3	256
15/10/2024	23	RNDM_0_5mm_0_2Hz	random	0.5	-	-	256
15/10/2024	24	T26_DH_pos_10%	DH	10%	-	-	256
15/10/2024	25	T26_DH_pos_20%	DH	20%	-	-	256
15/10/2024	26	T26_DH_pos_30%	DH	30%	-	-	256
15/10/2024	27	T26_DH_pos_50%	DH	50%	-	-	256
15/10/2024	28	T26_DH_pos_75%	DH	75%	-	-	256
15/10/2024	29	T26_DH_pos_100%	DH	100%	-	-	256
15/10/2024	30	T27_DH_neg_50%	DH	50%	-	-	256
15/10/2024	31	T27_DH_neg_100%	DH	100%	-	-	256
15/10/2024	32	T23_sine_150mm_0_265Hz_B	sine	150	250	3	256
15/10/2024	33	T26_DH_pos_100%_B	DH	100%	-	-	256
15/10/2024	34	T23_sine_150mm_0_265Hz_C	sine	150	250	3	256
15/10/2024	35	T23_sine_150mm_0_265Hz_D_neg	sine	150	250	3	256
16/10/2024	36	T19_sine_200mm_0_159Hz_D	sine	200	200	3	256
16/10/2024	37	T19_sine_200mm_0_159Hz_E	sine	200	200	2	256

4 Conclusion

This project involved an extensive experimental and numerical investigation aimed at evaluating the performance of sliding base-isolation bearings in real operating conditions. Full-scale static and dynamic in-situ tests were carried out on a base-isolated building that has been in service for approximately 15 years, providing unique insight into the long-term behavior of seismic isolation systems. The investigated structure, built within the C.A.S.E. Project following the 2009 L'Aquila earthquake, represents a highly significant case study for assessing the long-term performance and reliability of base-isolated buildings. The results highlight the importance of considering the variability and evolution of isolator properties over time, as well as their potential influence on the global seismic response of the structure.

The experimental campaign, performed using the EUCENTRE-IUSS mobile testing system MOBILAB, represents one of the first full-scale in-situ investigations specifically focused on quantifying the collective behavior of aged seismic isolation systems. The findings provide valuable information for evaluating whether existing base-isolated structures continue to meet the performance objectives prescribed by current Eurocode standards and for identifying possible improvements in future design, assessment, and maintenance procedures. The study contributed to addressing important research gaps related to aging and deterioration effects, dynamic interaction between the isolation system, substructure and superstructure, and the variability of mechanical properties among isolation devices across the isolation plane.

Overall, the project constitutes a significant contribution to international research in earthquake engineering, enhancing the understanding of the real-world performance of seismic isolation technologies and supporting the development of more reliable methodologies, technical standards, and resilient infrastructure design strategies.

A video of the test campaign can be found at this link:
https://youtu.be/xQtgx_ZMlH0?si=zjRA7kEsWBKhI2UA

References

[1] Calvi, P.M., Rapone, A., Becker, T.C., Sucuoglu, H., Gabbianelli, G., Chalarca, B., Lanese, I., O'Reilly, G.J., Rizzo-Parisi, E., Dacarro, F., 2026. Dynamic field testing of a 15-year-old friction pendulum base-isolated residential building. Soil Dynamics and Earthquake Engineering 200, 109802. https://doi.org/10.1016/j.soildyn.2025.109802

[2] Calvi GM, Spaziante V. Reconstruction between temporary and definitive: the CASE project. Progettazione Sismica 2009;3:221–50.

[3] Calvi GM. Mallet–Milne lecture 2025: risk management and rehousing of people displaced by earthquake disasters. Bull Earthq Eng 2025;23:2961–3041. https:// doi.org/10.1007/s10518-025-02141-w. 2025.

[4] ABAQUS. Analysis user's manual. 2022.

[5] CEN (Comit´e Europ´een de Normalisation). EN 15129: anti-seismic devices. Brussels: CEN; 2009. 2009.

[6] Norme Tecniche per le Costruzioni, NTC, 2018. Gazzetta Ufficiale, n. 42 del 20/02/2018, Supplemento ordinario n. 8.

Annex A

Instrumentation

Table 2: List of instruments.

Channel	Device Number	Order	Type	Range	Sensitivity [mV/g] accelerometer [mV/mm/Valim] pot	Notes	Orientation channel accelerometer
0	T1	53	POT	50mm	19.52	Pot Def trave 1	
1	T2	54	POT	50mm	19.44	Pot Def trave 2	
2	P1	55	POT	50mm	19.52	Slittamento trapezio 1-1	
3	P2	56	POT	50mm	19.55	Slittamento trapezio 1-2	
4	P3	57	POT	50mm	19.51	Slittamento trapezio 2-1	
5	P4	58	POT	50mm	19.51	Slittamento trapezio 2-2	
6	P5	59	POT	50mm	19.51	Abbassamento collare 1 - riscontro 2	
7	P6	60	POT	50mm	19.53	Slittamento trapezio 3-3	
8	P7	61	POT	50mm	19.45	Spostamento piastre isolatore riscontro 2 - poi trave4	
9	P8	62	POT	50mm	19.52	Slittamento trapezio 4-2	
10	P9	63	POT FILO	125mm	7.84	Spostamento colonna 1 (riscontro fisso)	
11	P10	64	POT FILO	125mm	7.75	Spostamento colonna 2 (riscontro fisso)	
12	T3	65	TAST	25mm	38.46	Spostamento verticale piastra S	
13	T4	66	TAST	25mm	37.63	Spostamento verticale piastra N	
14	P11	67	POT FILO	1000mm	0.95547	Spostamento piastra - giunto S	
15	P12	68	POT FILO	1000mm	0.95589	Spostamento piastra - giunto N	
16	P13	69	POT FILO	1000mm	0.95529	Spostamento piastra - frontale SO	
17	P14	70	POT FILO	1000mm	0.95498	Spostamento piastra - frontale NO	
18	P15	71	POT FILO	250mm	3.72	Spostamento laterale piastra NO	
19	P16	72	POT FILO	250mm	3.71	Spostamento laterale piastra SO	
20	ALIM	73	ALIM.	-	-	Alim.0:19 alimentazione canali da 0 a 19--alim1	
21	P19	74	POT	50mm	19.55	Spostam vert collare 1 - riscontro 2	
22	P20	75	POT	50mm	19.58	Spostam vert collare 2 - riscontro 2	
23	P21	76	POT	50mm	19.51	Spostam vert collare 3 - riscontro 2	

Table 3: List of instruments of external acquisition.

Channel	Device Number	Order	Type	Range	Sensitivity [mV/g] accelerometer [mV/mm/Valim] pot	Notes	Orientation channel accelerometer
0	P17	1	POT FILO	125mm	7.75	Drift solaio 1 - 1	X 2.7
1	P18	2	POT FILO	125mm	7.79	Drift solaio 1 - 2	
2	ALIM	3	ALIM.	-	-	Alim.0:1 alimentazione canali da 0 a 1--alim1	
3	Acc1 X	4	ACC3D	2g	1026.1	Acc1 X piastra NE	LONG
4	Acc1 Y	5	ACC3D	2g	1026.7	Acc1 Y piastra NE	TRANS_CF
5	Acc1 Z	6	ACC3D	2g	1019.7	Acc1 Z piastra NE	VERT_CF
6	Acc2 X	7	ACC3D	2g	1026.4	Acc2 X piastra SO	LONG
7	Acc2 Y	8	ACC3D	2g	1045.1	Acc2 Y piastra SO	TRANS_CF
8	Acc2 Z	9	ACC3D	2g	1008.6	Acc2 Z piastra SO	VERT_CF
9	Acc3 X	10	ACC3D	2g	1014.7	Acc3 X solaio 1 NE	LONG
10	Acc3 Y	11	ACC3D	2g	1004.2	Acc3 Y solaio 1 NE	TRANS_CF
11	Acc3 Z	12	ACC3D	2g	988.1	Acc3 Z solaio 1 NE	VERT_CF
12	Acc4 X	13	ACC3D	2g	993.8	Acc4 X solaio 1 SO	LONG
13	Acc4 Y	14	ACC3D	2g	998	Acc4 Y solaio 1 SO	TRANS_CF
14	Acc4 Z	15	ACC3D	2g	999.4	Acc4 Z solaio 1 SO	VERT_CF
15	Acc5 X	16	ACC3D	2g	1001.9	Acc5 X solaio 2 NE	LONG
16	Acc5 Y	17	ACC3D	2g	1016.6	Acc5 Y solaio 2 NE	TRANS_CF
17	Acc5 Z	18	ACC3D	2g	1003.1	Acc5 Z solaio 2 NE	VERT_CF
18	Acc6 X	19	ACC3D	2g	991.8	Acc6 X solaio 2 SO	LONG
19	Acc6 Y	20	ACC3D	2g	997.3	Acc6 Y solaio 2 SO	TRANS_CF
20	Acc6 Z	21	ACC3D	2g	981.5	Acc6 Z solaio 2 SO	VERT_CF
21	Acc7 X	22	ACC3D	6g	336.8	Acc7 X solaio 3 (sottotetto) NE	LONG
22	Acc7 Y	23	ACC3D	6g	336.5	Acc7 Y solaio 3 (sottotetto) NE	TRANS_CF
23	Acc7 Z	24	ACC3D	6g	330.3	Acc7 Z solaio 3 (sottotetto) NE	VERT_CF
24	Acc8 X	25	ACC3D	6g	328.9	Acc8 X solaio 3 (sottotetto) SO	LONG
25	Acc8 Y	26	ACC3D	6g	341.2	Acc8 Y solaio 3 (sottotetto) SO	TRANS_CF
26	Acc8 Z	27	ACC3D	6g	331	Acc8 Z solaio 3 (sottotetto) SO	VERT_CF
27	RO Forza	28	R.O.	-	400	R.O. Forza GdL	
28	RO Spost	29	R.O.	-	25	R.O. Spost GdL	

Table 4: List of instruments of external acquisition post test 7.

Channel	Device Number	Order	Type	Range	Sensitivity [mV/g] accelerometer [mV/mm/Valim] pot	Notes	Orientation channel accelerometer
0	P17	1	POT FILO	250mm	7.75	Drift solaio 1 - 1	X 2.7
1	P18	2	POT FILO	125mm	7.79	Drift solaio 1 - 2	
2	ALIM	3	ALIM.	-	-	Alim.0:1 alimentazione canali da 0 a 1--alim1	
3	Acc1 X	4	ACC3D	2g	1026.1	Acc1 X piastra NE	LONG
4	Acc1 Y	5	ACC3D	2g	1026.7	Acc1 Y piastra NE	TRANS_CF
5	Acc1 Z	6	ACC3D	2g	1019.7	Acc1 Z piastra NE	VERT_CF
6	Acc2 X	7	ACC3D	2g	1026.4	Acc2 X piastra SO	LONG
7	Acc2 Y	8	ACC3D	2g	1045.1	Acc2 Y piastra SO	TRANS_CF
8	Acc2 Z	9	ACC3D	2g	1008.6	Acc2 Z piastra SO	VERT_CF
9	Acc3 X	10	ACC3D	2g	1014.7	Acc3 X solaio 1 NE	LONG
10	Acc3 Y	11	ACC3D	2g	1004.2	Acc3 Y solaio 1 NE	TRANS_CF
11	Acc3 Z	12	ACC3D	2g	988.1	Acc3 Z solaio 1 NE	VERT_CF
12	Acc4 X	13	ACC3D	2g	993.8	Acc4 X solaio 1 SO	LONG
13	Acc4 Y	14	ACC3D	2g	998	Acc4 Y solaio 1 SO	TRANS_CF
14	Acc4 Z	15	ACC3D	2g	999.4	Acc4 Z solaio 1 SO	VERT_CF
15	Acc5 X	16	ACC3D	2g	1001.9	Acc5 X solaio 2 NE	LONG
16	Acc5 Y	17	ACC3D	2g	1016.6	Acc5 Y solaio 2 NE	TRANS_CF
17	Acc5 Z	18	ACC3D	2g	1003.1	Acc5 Z solaio 2 NE	VERT_CF
18	Acc6 X	19	ACC3D	2g	991.8	Acc6 X solaio 2 SO	LONG
19	Acc6 Y	20	ACC3D	2g	997.3	Acc6 Y solaio 2 SO	TRANS_CF
20	Acc6 Z	21	ACC3D	2g	981.5	Acc6 Z solaio 2 SO	VERT_CF
21	Acc7 X	22	ACC3D	6g	336.8	Acc7 X solaio 3 (sottotetto) NE	LONG
22	Acc7 Y	23	ACC3D	6g	336.5	Acc7 Y solaio 3 (sottotetto) NE	TRANS_CF
23	Acc7 Z	24	ACC3D	6g	330.3	Acc7 Z solaio 3 (sottotetto) NE	VERT_CF
24	Acc8 X	25	ACC3D	6g	328.9	Acc8 X solaio 3 (sottotetto) SO	LONG
25	Acc8 Y	26	ACC3D	6g	341.2	Acc8 Y solaio 3 (sottotetto) SO	TRANS_CF
26	Acc8 Z	27	ACC3D	6g	331	Acc8 Z solaio 3 (sottotetto) SO	VERT_CF
27	RO Forza	28	R.O.	-	400	R.O. Forza GdL	
28	RO Spost	29	R.O.	-	25	R.O. Spost GdL	

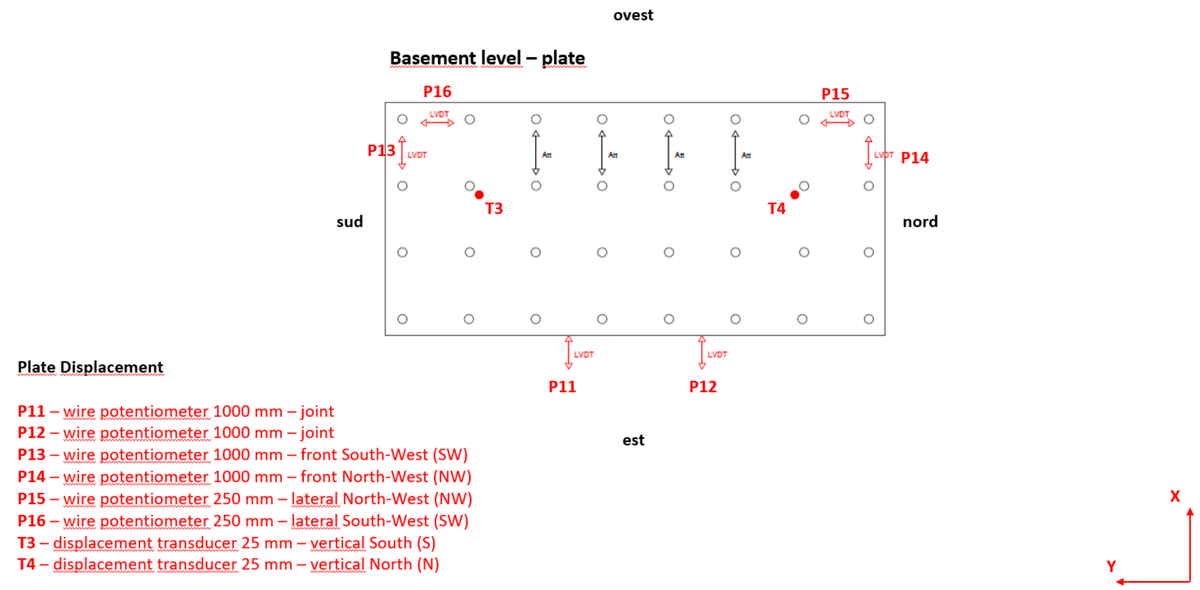

Figure 14: Instrumentation layout – basement level.

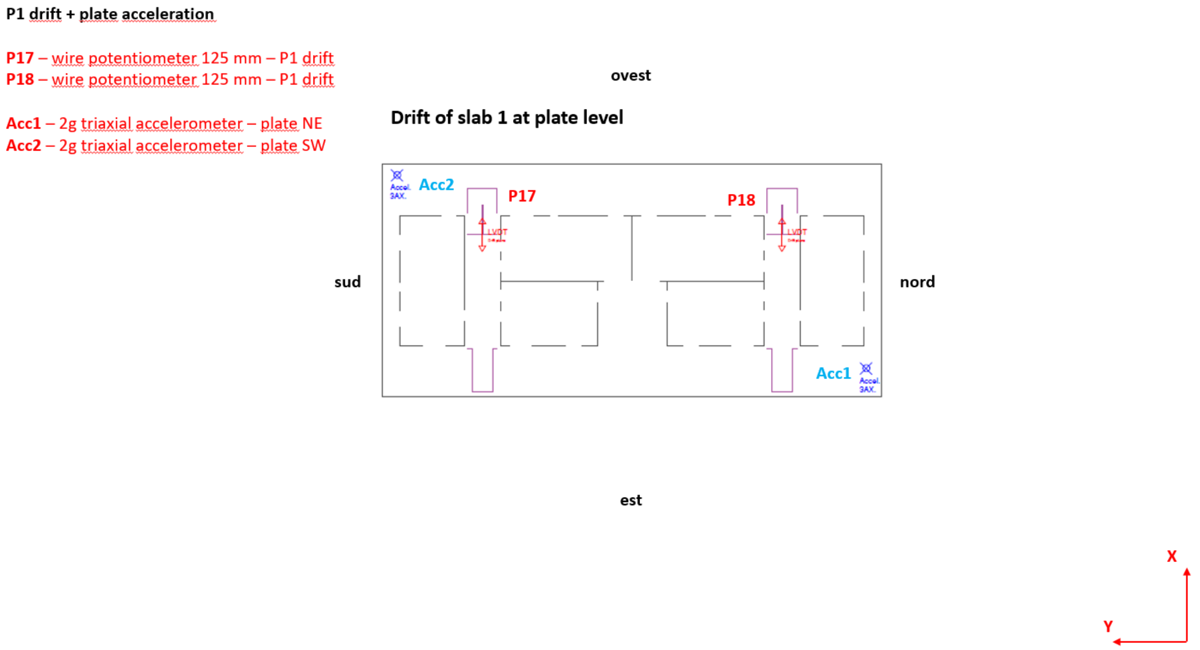

Figure 15: Instrumentation layout – plate level.

Slab 1 acceleration

Acc3 – 2g triaxial accelerometer – slab 1
Acc4 – 2g triaxial accelerometer – slab 1

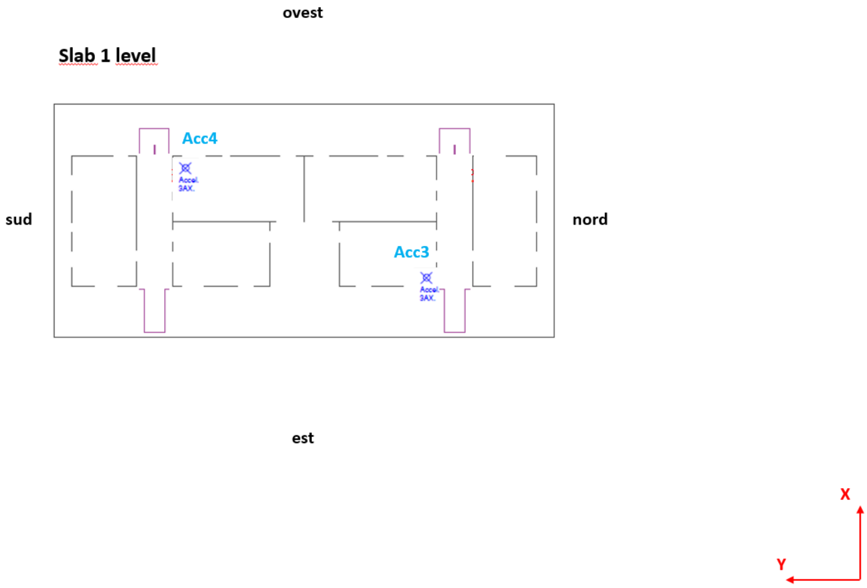

Figure 16: Instrumentation layout – slab level 1.

Slab 2 acceleration

Acc5 – 2g triaxial accelerometer – slab 2
Acc6 – 2g triaxial accelerometer – slab 2

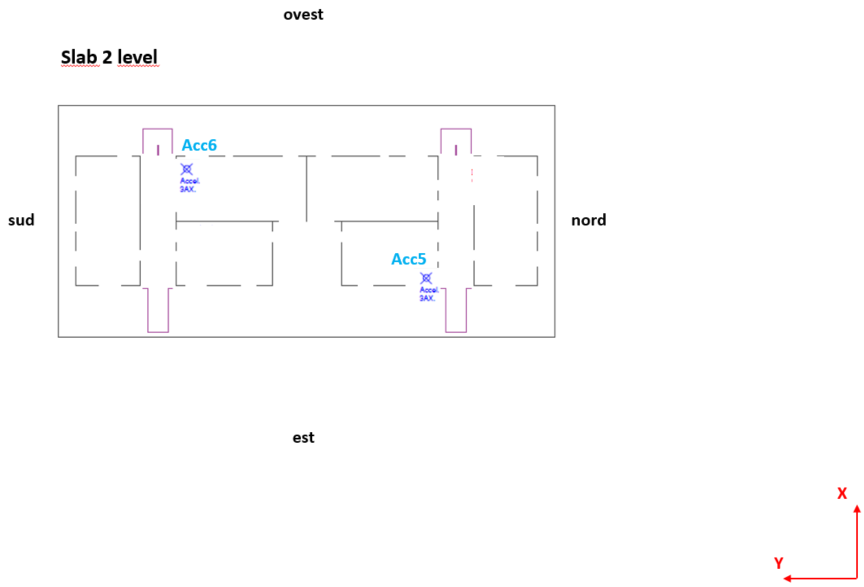

Figure 17: Instrumentation layout – slab level 2.

Slab 3 acceleration (attic)

Acc7 – 6g triaxial accelerometer – slab 3
Acc8 – 6g triaxial accelerometer – slab 3

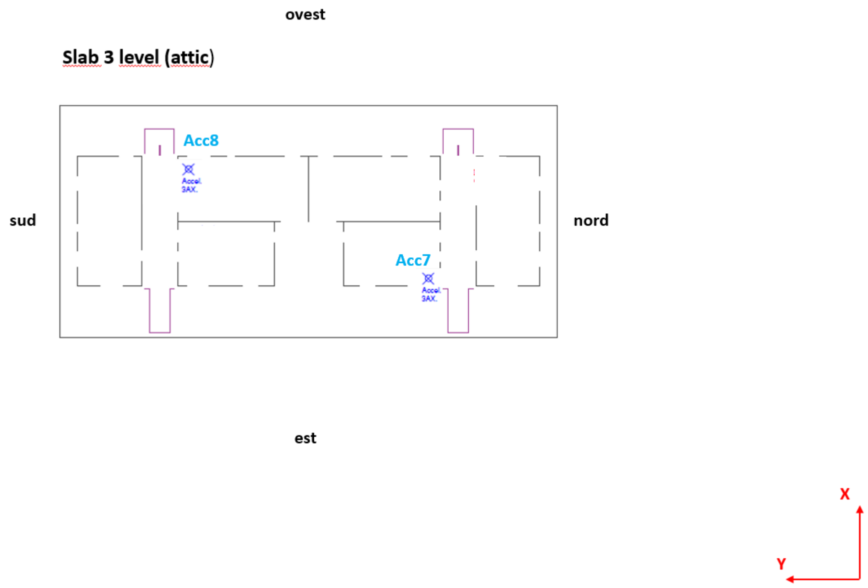

Figure 18: Instrumentation layout – slab level 3.